Journal of
Materials Chemistry A

Accepted Manuscript

This article can be cited before page numbers have been issued, to do this please use: C. Sun, C. A. López and J. A. Alonso, *J. Mater. Chem. A*, 2017, DOI: 10.1039/C7TA01404J.

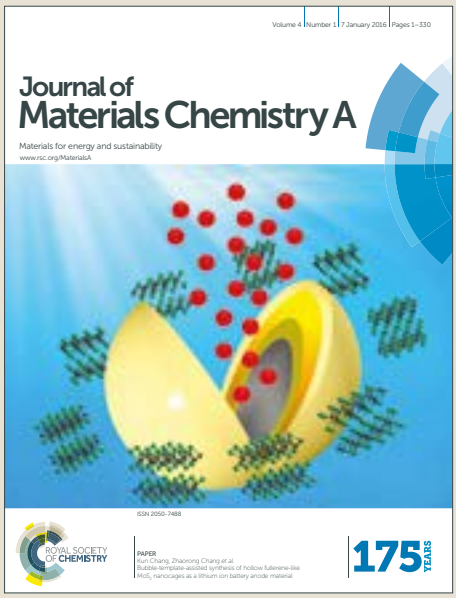

ROYAL SOCIETY OF CHEMISTRY

rsc.li/materials-a

View Article Online
DOI: 10.1039/C7TA01404J

Elucidating the Diffusion Pathway of Protons in Ammonium Polyphosphate: a potential Electrolyte for Intermediate Temperature Fuel Cells

Chunwen Sun,[†*] Carlos Alberto López[‡] and José Antonio Alonso[⊥*]

[†] *Beijing Institute of Nanoenergy and Nanosystems, Chinese Academy of Sciences; National Center for Nanoscience and Technology (NCNST), Beijing 100083, China*

[‡] *INTEQUI, Universidad Nacional de San Luis, CONICET, Fac. Qca., Bqca. y Far. (Chacabuco y Pedernera, 5700), San Luis, Argentine*

[⊥]*Instituto de Ciencia de Materiales de Madrid, CSIC, Cantoblanco 28049 Madrid, Spain*

[*] Corresponding authors.

Tel: +86-10-82854648, Fax: +86-10-82854648, Email: sunchunwen@binn.cas.cn (C. Sun),

Tel: +34-91-3349071, Fax: +34-91-3720623, Email: ja.alonso@icmm.csic.es (J.A. Alonso)

View Article Online
DOI: 10.1039/C7TA01404J

ABSTRACT

Ammonium polyphosphate (NH_4PO_3) is a potential electrolyte material for intermediate temperature fuel cells (150-250^oC). The crystal structure of NH_4PO_3, including the H positions, is unravelled from neutron powder diffraction (NPD) data by successive Fourier synthesis from the polyphosphate backbone. The structure consists of zig-zag chains aligned along [001] directions of tetrahedral phosphate PO_4 units that are connected through O3 atoms with P–O3–P angles of 126.3(5) °. The proton conductivity mechanism of NH_4PO_3 is clarified from the thermal evolution of the structure. It shows that some H atoms subtly shift at high temperatures, resulting in a weakening of certain H-bonds, thus increasing the lability of those H involved in the proton conduction mechanism. Conductivity measurements in humid air and H_2 for NH_4PO_3 show high proton conductivities of 1.2×10^{-5}~2.61×10^{-3} S cm^{-1} and 2.2×10^{-5}~2.69×10^{-3} S cm^{-1}, respectively, in the temperature range from 50 ^oC to 275 ^oC.

KEYWORDS.

Ammonium polyphosphate, proton conductivity, neutron powder diffraction, intermediate temperature fuel cells

View Article Online
DOI: 10.1039/C7TA01404J

1. Introduction

Fuel cells have attracted worldwide attention as a clean power source due to their high efficiency in energy conversion and low emissions.[1-3] Polymer membranes, like Nafion®, are still the main electrolyte component for low-temperature fuel cells. However, their operating temperatures are usually limited below the boiling point of water, 100 ℃. At these temperatures, CO poisoning is a severe problem if the cell is operated on carbon based fuels. Furthermore, high loadings of noble metal catalysts are required to compensate for the low catalytic activity and internal CO poisoning.[4] Numerous oxide ionic conductors for solid oxide fuel cells operating above 600^{o}C such as scandia-stabilized zirconia (ScSZ), lanthanum strontium gallium magnesium oxide (LSGM), gadolinia-doped ceria (GDC), show high ionic conductivities, but mainly based on oxide ion conducting.[5] Solid acids, like $CsHSO_4$, were proposed for applications at temperature up to 160 ^{o}C and not affected by humid atmospheres. However, their disadvantage is their solubility in water.[6]

In recent years, considerable effort has been devoted toward the development of solid-state proton conductors capable of operating in the intermediate temperature range of 150 to 400 ^{o}C due to their advantages over perfluorosulfonic or sulfonated aromatic polymer electrolyte.[4,6-9] A possible candidate to replace Nafion® is ammonium polyphosphate (hereafter abbreviated as NH_4PO_3) based electrolytes.[4,10,11] However, to our knowledge no information on the H positions in NH_4PO_3 has been reported until now.

Herein, we have prepared NH_4PO_3 by a solid-state reaction. The crystal structure of NH_4PO_3 and its temperature dependent structural evolution were investigated by neutron powder diffraction (NPD) experiments as well as X-ray diffraction (XRD). The relationship between the structure and conductivity property of NH_4PO_3 as a proton conductor for intermediate temperature fuel cells (ITFCs) has been established, and the microscopic reason for the observed good performance has been unveiled.

2. Experimental

Ammonium polyphosphate with crystalline form II was prepared as reported previously.[12]

View Article Online
DOI: 10.1039/C7TA01404J

X-ray powder diffraction (XPRD) patterns were obtained on a Bruker-AXS D8 diffractometer with Cu Kα radiation in the 2θ range from 5 ° up to 120 ° with increments of 0.02 °. Neutron powder diffraction (NPD) patterns were collected at the HRPT diffractometer of the SINQ spallation source (PSI, *Paul Scherrer Institute*, Villigen, Switzerland) with a wavelength of 1.494 Å at room temperature (RT), 100 and 200 ℃. Both XRPD and NPD diffraction patterns were analysed with the Rietveld method using the *FullProf* program.[13,14] The coherent scattering lengths for P, O, N and H were 5.13, 5.803, 9.36 and -3.739 fm, respectively.

For impedance spectra measurements, the obtained ammonium polyphosphate powder were pressed at 510 MPa into pellets. The pellets are 1 cm in diameter. The thickness of the pellets is in the range of 1-1.6 mm. Then the pellets were sputtered gold using a machine (Sputter Coater SCD 004, BALZERS). The gold-sputtered pellets were placed in a home-made four electrode apparatus and placed in a furnace for the impedance measurements, which were performed with a Solartron 1260 Impedance/Gain-Phase Analyzer in combination with a 1286 Electrochemical Interface. The pellet was fixed between two platinum wire meshes. The frequency range is from 1 Hz to 1 MHz. The temperature was measured using a NiCr–Ni thermocouple type K in contact with the pellet. The measurement was carried out in humid air and hydrogen. The impedance spectra were recorded at constant temperatures after 1 h equilibration time. The data were analyzed using a ZView software (version 2.1).

3. Results and Discussion

Structural characterizations of NH_4PO_3

The structural characterization of NH_4PO_3 was initially performed from XRPD data at RT and refined using the Rietveld method. Several polymorphic phases of this compound have been reported in the last 45 years.[15-17] According to an initial analysis, the XRPD pattern matches with the form II. Crystal structure of this polymorph was reported in 1994 by Brühne *et. al.*.[18] This is the unique crystal structure described hitherto, performed from XRPD in the $P2_12_12_1$space group with the following unit-cell parameters: *a*=12.079(1),

View Article Online
DOI: 10.1039/C7TA01404J

b=6.4887(8) and *c*=4.2620(4) Å. However, no information on the H positions has been reported so far.

This crystallographic model was used to refine our XRPD pattern by the Rietveld method. Fig. 1 shows the best fit of the XRPD pattern and Table S1 (Supporting information) shows the atomic parameters for P, O and N atoms. Despite the good quality of the refinement, the hydrogen positions cannot be located from XRPD. For this reason, NPD data were collected at RT, 100 and 200 ℃ with the aim to unveil the hydrogen positions, which are of paramount importance to describe and understand the proton conductivity behaviour of this material. In the initial model defined in the $P2_12_12_1$ (N°19) space group,[18] P, N and three types of oxygen O1, O2 and O3 are all placed at general 4*a* (x,y,z) positions. The unit-cell parameters at RT from NPD data are *a*=12.049(1) Å, *b*=6.4709(5) Å, *c*=4.2486(4) Å and V = 331.26(5) Å^3 in good agreement with the literature. This model gave a very poor fit to the neutron data, since the contribution of the H atoms is very important. At this point, it was possible to locate the H positions by performing a difference Fourier synthesis from the observed and calculated NPD data for the previous model. The difference contains information of the missing scattering density (in this case nuclear density).

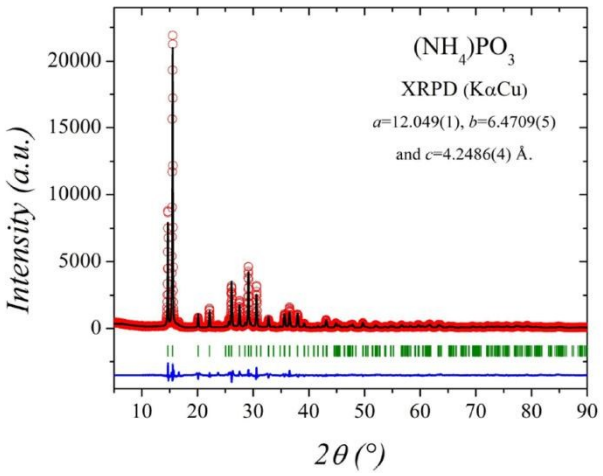

Fig. 1 Observed (circles), calculated (line), and difference (bottom) XRD patterns of the NH_4PO_3 at room temperature.

View Article Online
DOI: 10.1039/C7TA01404J

Fig. 2 illustrates a difference Fourier map of the *z*= 0.43 section, where strong negative peaks were observed at (0.08, -0.03, 0.43). These peaks were assigned to H1 atoms, since H has negative scattering length for neutrons. H1 was then introduced in the structural model and its occupancy and thermal factor were refined; this leads to a significant improvement of the profile fit and reduction of the discrepancy factors. The four types of independent H atoms (H1, H2, H3 and H4) were located by successive Fourier synthesis and introduced in the structural model, dramatically improving the quality of the fit.

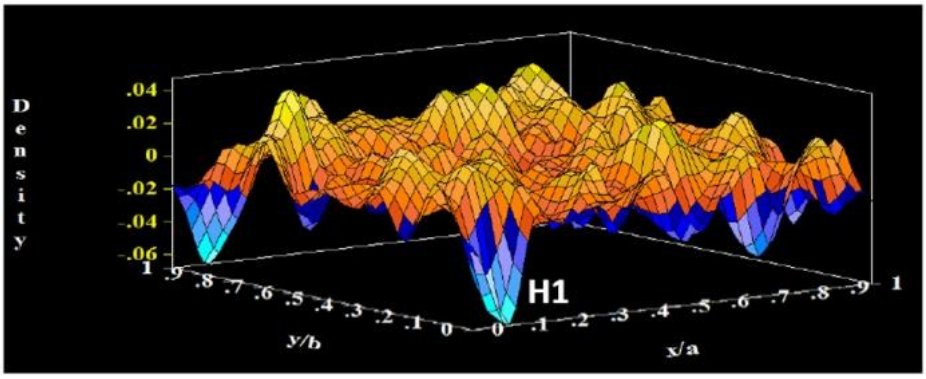

Fig. 2 Difference Fourier map of the *z*= 0.43 section, where strong negative peaks were observed at (0.08, -0.03, 0.43).

A further step was adopted to consider the several chemical geometries that are well known for PO_4 and NH_4 groups, which can be used to constrain the structural parameters in order to improve the atomic positions refinement. P in the phosphate group has a sp^3 hybridization, which implies a chemical constrains with tetrahedral geometry. The same constraint is presented in ammonium groups where nitrogen atoms also have a sp^3 hybridization. From these molecular features, several geometric restraints concerning distances and angles might be used. However, in the present case only the H-N-H angles were constrained to the tetrahedral form in ammonium groups, to 109.5 °. An important remark is that a constrained parameter is not limited between two end values; instead each constrain with its standard deviation is included in the function to be minimized in the Rietveld method. All instrumental and atomic parameters were refined until reaching the convergence. Fig. 3 shows the good agreement between the observed and calculated NPD

View Article Online
DOI: 10.1039/C7TA01404J

patterns after the final refinement at RT. The Rietveld fits at 100 and 200 ℃ are shown in Fig. S1 (Supporting information). The high level of background is due to the incoherent scattering from H in the present non-deuterated sample, which was not an obstacle to properly refine the crystal structure parameters.

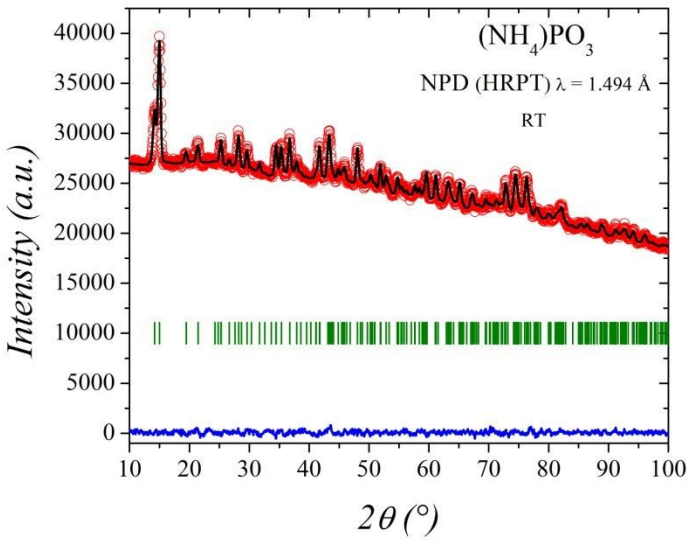

Fig. 3 Observed (circles), calculated (line), and difference (bottom) neutron-diffraction patterns of the NH_4PO_3 at room temperature.

The atomic parameters determined from NPD data at RT, are included in Table 1, whereas those corresponding to 100 and 200 ℃ are listed in Table S2. The main bond distances and angles are given in Table 2. Fig. 4 shows two schematic views of crystal structure obtained at RT from the NPD refinement along [001] and [100] directions, where the most characteristic features may be observed. The tetrahedral phosphate PO_4 units are connected through O3 atoms forming the zig-zag chains aligned along [001] directions. The P–O3–P angle within the chains are of 126.3(5) °, 126.4(6) ° and 127.3(6) ° for RT, 100 ℃ and 200 ℃, respectively. The ammonium NH_4^+ groups are distributed between these chains, bonded to the polyphosfate backbone through H-bond interactions (N–H···O–P). The dashed lines in Fig. 4a indicate the H-bond interactions. The most important H-bond interactions (distance, angle and type of H-bridge) are listed in Table 3. There are two types

View Article Online
DOI: 10.1039/C7TA01404J

of hydrogen bridges: normal and bifurcated H-bonds. Taking into account the classification of Jeffrey for H-bonds[16] and the parameters listed in Table 3, the observed interactions in this compound are ranked between moderate and weak.

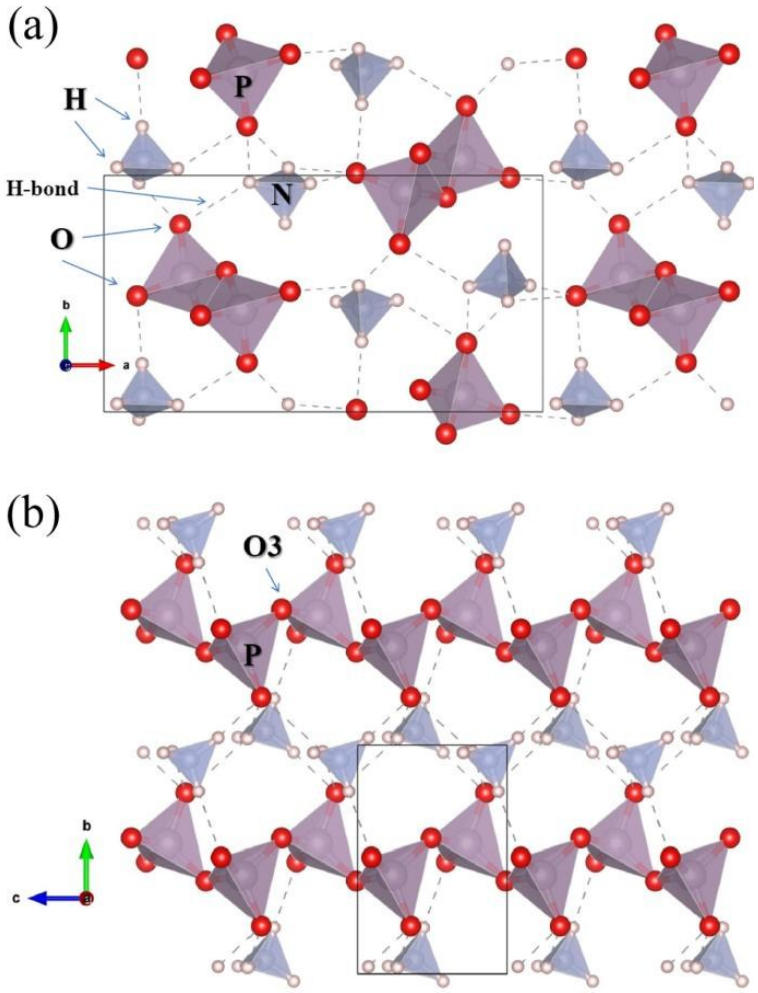

Fig. 4 Schematic view of the crystal structure of the NH_4PO_3 obtained at RT from the NPD refinement along (a) [001] and (b) [100] directions.

The high-temperature evolution of the structure also reveals interesting features. As the temperature increases up to 200 ℃, a normal evolution in the unit-cell parameters and selected distances and angles are observed, as shown in Table 3. However, some subtle changes in the H-bond interactions must be highlighted. Some selected H-bonds show a weakening upon heating, within standard deviations. Considering the previously mentioned

View Article Online
DOI: 10.1039/C7TA01404J

classification of Jeffrey for H-bond[19] the H-bonds for H1 and H2 become weaker, as illustrated in Fig. 5, a sequence of the ammonium evolution with temperature is shown.

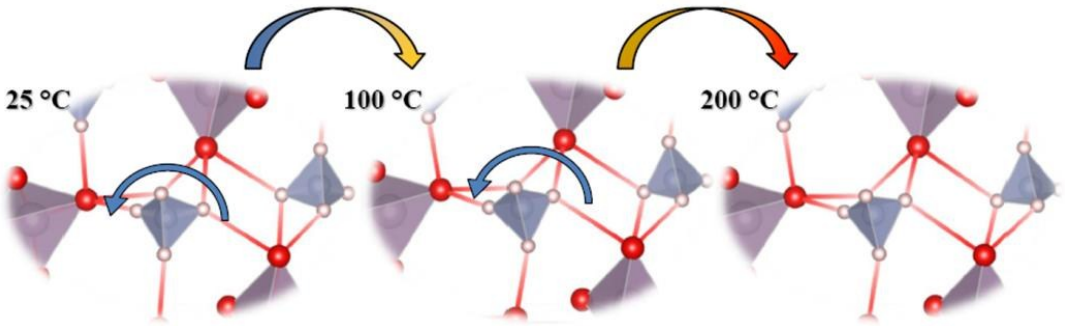

Fig. 5 The ammonium evolution in NH_4PO_3 versus temperature.

Analysing the geometries of the H-bond interactions, the hydrogen mobility can be promoted by an intermediate protonated phosphate group, as the following equilibrium:

This intermediate group probably decreases the activation energy of the proton jump between ammonium groups, explaining the motion between adjacent NH_4^+ units. This mechanism implies that the neighbouring unit is in the ammonia form (NH_3) to be able to accept and accommodate the H^+. On the other hand, the oxygen atoms are too far apart (≈4.25 Å) to allow the H^+ to jump between two adjacent oxygen atoms. Moreover, for an effective proton conductivity, as exhibited by this compound, the hydrogen atoms should be delocalised around nitrogen atoms. In order to visualize this phenomenon, difference Fourier maps were obtained for a structural model without hydrogen atoms. The negative iso-surface obtained was over-imposed on the refined structure at RT and 200 ℃, as displayed in Fig. 6. The delocalization of hydrogen atoms is clearly unveiled in these Figures; this fact demonstrates that each proton is easily exchanged with their neighbours.

View Article Online
DOI: 10.1039/C7TA01404J

The shape of the negative density patches also accounts for the high displacement factors obtained for H atoms. Besides the great proton delocalization observed in ammonium groups, Fig. 5 also reveals an increase in the number of isolated negative densities between the ammonium groups at 200 ℃. The distance of these negative regions to oxygen atoms are in the range to those expected for H–O=P bonds. These negative patches probably indicate intermediate positions occupied during the proton motion process, visualizing the H diffusion paths at an elevated temperature, when the ionic conductivity is highly enhanced, as experimentally observed.

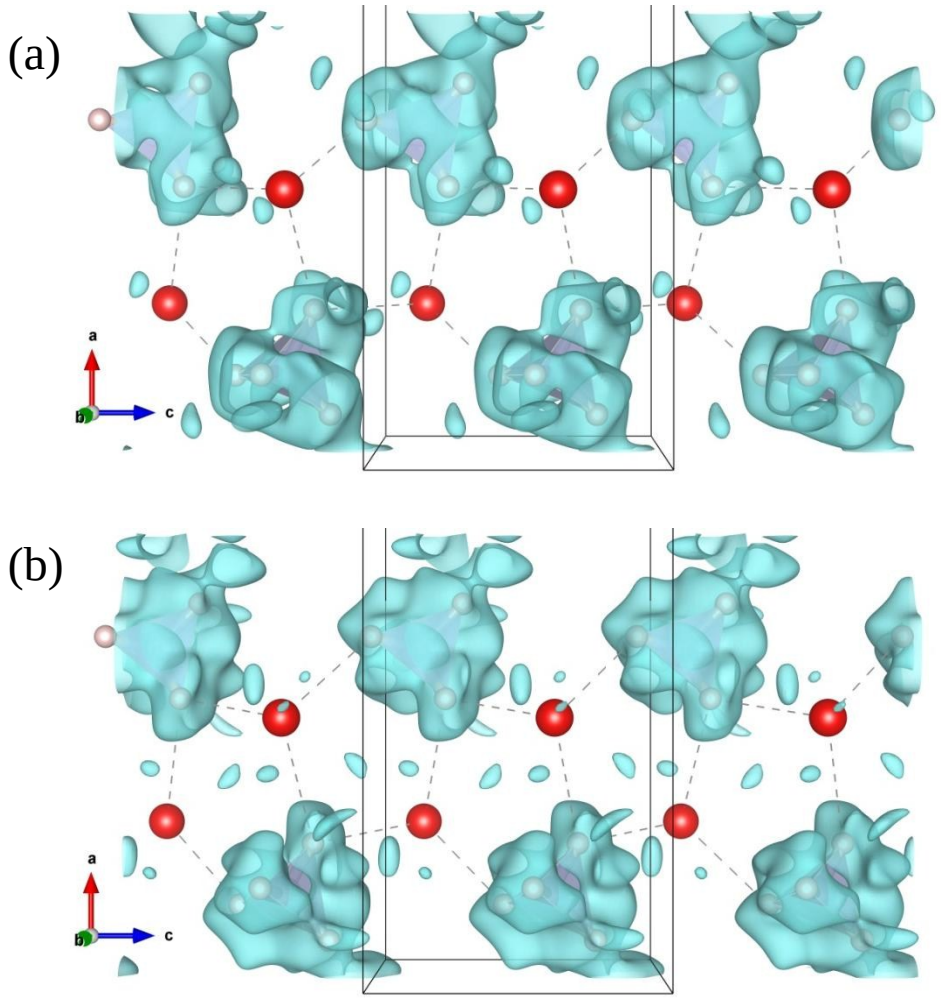

Fig. 6 The delocalization of hydrogen atoms in NH_4PO_3 at (a) RT and (b) 200 ℃.

View Article Online
DOI: 10.1039/C7TA01404J

The temperature dependence of the proton conductivity of NH_4PO_3 is displayed in Fig. 7. It shows that NH_4PO_3 exhibits high proton conductivities of 1.2×10^{-5}~2.61×10^{-3} S cm^{-1} and 2.2×10^{-5}~2.69×10^{-3} S cm^{-1} in humid air and H_2 in the temperature range from 50 ^{o}C to 275 ^{o}C, respectively. The conductivity of NH_4PO_3 is comparable to that of propanesulfonated polybenzimidazole (PBI-PS) (~0.00158 S cm^{-1} at 140^{o}C).[3] From the practical point of view, heterogeneous doping of ionic salts with highly dispersed oxides, such as Al_2O_3, TiO_2, SiO_2, was found to be an effective method to further enhance the ionic conductivity.[4,20,21] These results demonstrate that NH_4PO_3 is a promising electrolyte material for intermediate temperature fuel cells.

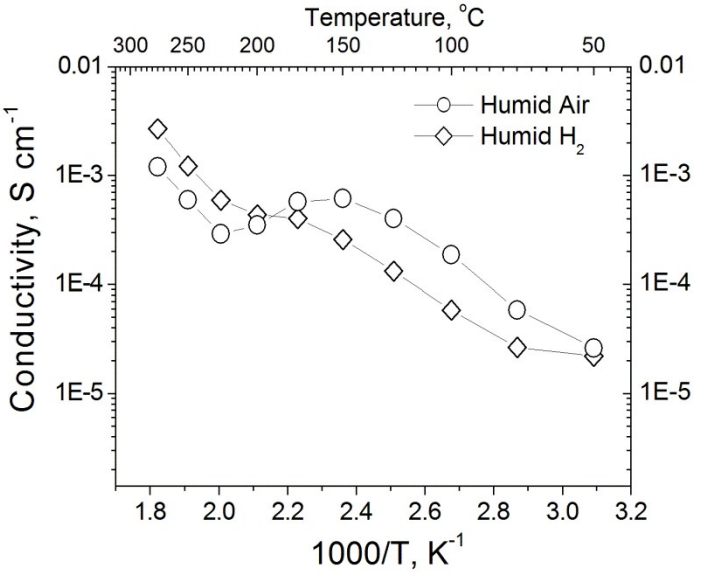

Fig. 7 Temperature dependent of the proton conductivity of NH_4PO_3.

4. Conclusions

The crystal structure of ammonium polyphosphate was completely resolved from a NPD study, by successive Fourier synthesis from the polyphosphate backbone. The structure consists of zig-zag chains aligned along [001] directions of tetrahedral phosphate PO_4 units that are connected through O3 atoms with P–O3–P angles of 126.3(5) ° at RT. The ammonium NH_4 groups are located between these chains, bonded to the polyphosphate backbone through H-bond interactions (N–H···O–P). The thermal evolution of the structure

View Article Online
DOI: 10.1039/C7TA01404J

shows that some H atoms subtly shift at high temperatures, resulting in a weakening of certain H-bonds, thus increasing the lability of those H involved in the proton conduction mechanism.

ACKNOWLEDGEMENTS

C.S. acknowledges the financial support of the National Natural Science Foundation of China (Nos. 51372271 and 51672029). This work was also supported by National Key R & D Project from Ministry of Science and Technology, China (2016YFA0202702) and the *Thousands Talents Program* for the pioneer researcher and his innovation team in China. J.A.A. acknowledges the Spanish Ministry of Economy and Competitivity for granting the project MAT2013-41099-R. C.A.L. acknowledges ANPCyT for financial support (project PICT2014-3576). The authors thank the PSI (Switzerland) for making all facilities available for the neutron diffraction experiments.

References

1 B.C.H. Steele, A. Heinzel, Materials for fuel-cell technologies, *Nature* **2001**, 414, 345-352.

2 C. W. Sun, U. Stimming, Recent anode advances in solid oxide fuel cells, *J. Power Sources* 2007, *171*, 247-260.

3 Q. Li, R. He, J.O. Jensen, N.J. Bjerrum, Approaches and recent development of polymer electrolyte membranes for fuel cells operating above 100^{o}C, *Chem. Mater.* **2003**, *15*, 4896-4915.

4 C.W. Sun, U. Stimming, Synthesis and characterization of NH_4PO_3 based composite with superior proton conductivity for intermediate temperature fuel cells, *Electrochim. Acta* **2008**, *53*, 6417-6422.

5 C. W. Sun, R. Hui, J. Roller, Cathode materials for solid oxide fuel cells: a review, *J. Solid State Electrochem* 2010, *14*, 1125-1143.

6 S. M. Haile, D.A. Boysen, C.R.I. Chisholm, R.B. Merle, Solid acids as fuel cell electrolytes, *Nature* **2001**, *410*, 910-913.

View Article Online
DOI: 10.1039/C7TA01404J

7 G. Alberti, M. Casciola, Composite membranes for medium-temperature PEM fuel cells, *Annu. Rev. Mater. Res.* 2003, *33*, 129-154.

8 A. Goni-Urtiaga, D. Presvytes, K. Scott, Solid acids as electrolyte materials for proton exchange membrane (PEM) electrolysis: Review, *Int. J. Hydrogen Energy* 2012, *37*, 3358-3372.

9 M. Nagao, A. Takeuchi, P. Heo, T. Hibino, M. Sano, A. Tomita, A proton-conducting In^{3+}-doped SnP_2O_7 electrolyte for intermediate-temperature fuel cells, *Eletrochem. Solid-state Lett.* **2006**, *9*, A105-A109.

10 O. Paschos, J. Kunze, U. Stimming, F. Maglia, A review on phosphate based, solid state, protonic conductors for intermediate temperature fuel cells, *J. Phys.: Condens. Mater.* **2011**, *23*, 234110.

11 M. Cappadonia, O. Niemzig, U. Stimming, Preliminary study on the ionic conductivity of a polyphosphate composite, *Solid State Ionics* **1999**, *125*, 333-337.

12 G. S. Liu, X. C. Liu and J. G. Yu, Ammonium Polyphosphate with Crystalline Form V by Ammonium Dihydrogen Phosphate Process, *Ind. Eng. Chem. Res.* **2010**, *49*, 5523–5529.

13 H. M. Rietveld, A profile refinement method for nuclear and magnetic structures, *J. Appl. Crystallogr.* **1969**, *2*, 65–71.

14 J. Rodr ǵuez-Carvajal, Recent advances in magnetic-structure determination by neutron powder diffraction, *Phys. B* **1993**, *192*, 55-69.

15 C. Y. Shen, N. E. Stahlheber and D. R. Dyroff, Preparation and Characterization of Crystalline Long-chain Ammonium Polyphosphates, *J. Am. Chem. Soc.* **1996**, *91*, 62.

16 G. X. Zhao and G. S. Liu, Ammonium Polyphosphate with Crystal Form V by DAP+P_2O_5, *Adv. Mater. Res.* **2011**, *306-307*, 713-716.

17 D. T. Pan, J. W. Zhu, Y. Y. Wu, K. Chen, B. Wu and L. J. Ji, Study on the Crystal Transformation of Ammonium Polyphosphate Crystalline Form V, Phosphorous, Sulpure, and Silicon and the Related Elements, **2016**, 191, 1306-1312.

18 B. Bruhne and M. Jansen, Crystal Structure Determination of Ammonium catena-Polyphosphate I1 by X-Ray Powder Techniques, *Z. anorg. allg. Chem.* **1994**, *620*, 931-935.

View Article Online
DOI: 10.1039/C7TA01404J

19 G. A. Jeffrey, An Introduction to Hydrogen Bonding, Oxford University Press, Oxford, **1997**.

20 C.C. Liang, Conduction characteristics of lithium iodide aluminum oxide solid electrolytes, *J. Electrochem. Soc.* **1973**, *120*, 1289-1292.

21 J. Maier, Ionic-conduction in space charge regions, *Prog. Solid State Chem.* **1995**, *23*, 171-263.

View Article Online
DOI: 10.1039/C7TA01404J

Table 1. Crystallographic data for NH_4PO_3 phase from NPD at RT. System: orthorhombic, Space group: $P2_12_12_1$.

a) RT. Unit-cell parameters: a=12.047(2) Å, b=6.4721(8) Å, c=4.2498(6) Å and V = 331.34(8) Å^3.					
Atom	x/a	y/b	z/c	B_{iso}	Occ
P	0.1866(9)	0.568(2)	0.270(2)	1.3(2)	1
O1	0.174(1)	0.790(1)	0.145(3)	1.7(1)	1
O2	0.0758(9)	0.490(1)	0.408(2)	1.8(1)	1
O3	0.2800(9)	0.593(2)	0.509(2)	1.8(1)	1
N	0.0898(6)	0.062(1)	0.622(1)	2.0(2)	1
H1	0.080(2)	-0.032(5)	0.428(7)	8.4(4)	1
H2	0.168(3)	0.028(5)	0.734(6)	8.4(4)	1
H3	0.030(2)	0.034(6)	0.794(6)	8.4(4)	1
H4	0.087(3)	0.203(5)	0.560(8)	8.4(4)	1
R_p: 0.7%; R_{wp}: 0.9%; R_{exp}: 0.6%; χ^2: 1.9; R_{Bragg}: 7.1%					

Table 2. Main interatomic distances (Å) and angles (°)

	RT	100 ℃	200 ℃
Phosphorus tetrahedrons			
P–O1	1.54(2)	1.56(2)	1.54(2)
P–O2	1.54(2)	1.51(2)	1.50(2)
P–O3	1.58(1)	1.60(3)	1.64(2)
P–O3’	1.52(2)	1.54(2)	1.54(2)
<P–O>	1.54	1.55	1.56
P–O3–P’	126.3(5)	126.4(6)	127.3(6)
Ammonia tetrahedrons			
N–H1	1.03(4)	0.94(4)	0.89(4)
N–H2	1.08(4)	0.95(4)	0.99(4)
N–H3	1.04(3)	1.09(3)	1.03(4)
N–H4	0.95(4)	1.01(5)	1.04(4)
<N–H>	1.03	1.00	0.99

View Article Online
DOI: 10.1039/C7TA01404J

Table 3. Distances (Å) and angles (°) for the main H-bond interactions.

	RT		100 ℃		200 ℃		Type of H-bridges
H-bond	Distance	Angle	Distance	Angle	Distance	Angle	
N–H1···O1	2.01(4)	138.7(7)	2.15(4)	133(1)	2.26(4)	131(1)	Bifurcated
N–H1···O2	2.36(3)	122.5(7)	2.34(4)	129.3(9)	2.34(4)	134(1)	Bifurcated
N–H2···O1	2.27(4)	123.6(7)	2.27(4)	131.7(9)	2.24(4)	133.6(9)	Bifurcated
N–H2···O1’	2.33(4)	119.5(8)	2.42(4)	116.2(8)	2.46(4)	113.2(8)	Bifurcated
N–H3···O2	1.82(3)	179(1)	1.86(4)	166(1)	1.84(4)	172(1)	Normal
N–H4···O2	1.97(4)	176.5(9)	1.94(5)	162(1)	1.94(5)	162.5(8)	Normal

View Article Online
DOI: 10.1039/C7TA01404J

Table of Contents (TOC)

The Diffusion Pathway of Protons in Ammonium Polyphosphate is revealed.